

Antideuteron Production in 158A GeV/c Pb + Pb Collisions

I. G. Bearden,¹ H. Bøggild,¹ J. Boissevain,² P. H. L. Christiansen,¹ L. Conin,³ J. Dodd,⁴ B. Erasmus,³ S. Esumi,^{5,*} C. W. Fabjan,⁶ D. Ferenc,⁷ A. Franz,^{6,†} J. J. Gaardhøje,¹ A. G. Hansen,¹ O. Hansen,¹ D. Hardtke,^{8,‡} H. van Hecke,² E. B. Holzer,⁶ T. J. Humanic,⁸ P. Hummel,⁶ B. V. Jacak,⁹ K. Kaimi,^{5,§} M. Kaneta,⁵ T. Kohama,⁵ M. L. Kopytine,⁹ M. Leltchouk,⁴ A. Ljubicic,⁷ B. Lörstad,¹⁰ L. Martin,³ A. Medvedev,⁴ M. Murray,¹¹ H. Ohnishi,^{5,†} G. Paic,⁶ S. U. Pandey,^{8,||} F. Piuz,⁶ J. Pluta,^{3,**} V. Polychronakos,¹² M. Potekhin,⁴ G. Poulard,⁶ D. Reichold,⁸ A. Sakaguchi,^{5,††} J. Schmidt-Sørensen,¹⁰ J. Simon-Gillo,² W. Sondheim,² T. Sugitate,⁵ J. P. Sullivan,² Y. Sumi,⁵ W. J. Willis,⁴ K. L. Wolf,^{11,§} N. Xu,^{2,‡} and D. S. Zachary⁸

¹Niels Bohr Institute, DK-2100, Copenhagen, Denmark

²Los Alamos National Laboratory, Los Alamos, New Mexico 87545

³Nuclear Physics Laboratory of Nantes, 44072 Nantes, France

⁴Columbia University, New York, New York 10027

⁵Hiroshima University, Higashi-Hiroshima 739, Japan

⁶CERN, CH-1211 Geneva 23, Switzerland

⁷Rudjer Bosovic Institute, Zagreb, Croatia

⁸Ohio State University, Columbus, Ohio 43210

⁹SUNY at Stony Brook, Stony Brook, New York 11794

¹⁰University of Lund, S-22362 Lund, Sweden

¹¹Texas A&M University, College Station, Texas 77843

¹²Brookhaven National Laboratory, Upton, New York 11973

(Received 5 November 1999)

The invariant cross section as a function of transverse momentum for antideuterons produced in 158A GeV/c per nucleon Pb + Pb central collisions has been measured by the NA44 experiment at CERN. This measurement, together with a measurement of antiprotons, allows for the determination of the antideuteron coalescence parameter. The extracted coalescence radius is found to agree with the deuteron coalescence radius and radii determined from two particle correlations.

PACS numbers: 25.75.Dw, 13.85.-t, 14.20.Dh, 25.40.Ve

In central collisions of heavy ions, e.g., Pb + Pb, at ultrarelativistic energies, a region of highly compressed and heated nuclear matter is formed. This region subsequently expands both along and transverse to the beam direction until the constituent particles cease to interact at freeze-out. In order to be able to derive characteristic energy and matter densities, it is important to determine the spatial extent and the density profile of the expanding source at the time of freeze-out. Such information has so far come primarily from Hanbury-Brown and Twiss (HBT) interferometry, where the extent of the source can be estimated from the dependence of the two particle correlation function on the relative momentum of the two particles (e.g., $\pi - \pi$ [1,2]). Interpretation of HBT data normally relies on assumptions on the density profile of the emitting source.

Independent information on source characteristics can be obtained from a different two body correlation, namely, the formation of deuterons and antideuterons. As a consequence of the small binding energy of the deuteron (2.2 MeV) compared to typical kinetic energies of the particles in the fireball, deuterons can survive only when the probability for collisions within the expanding source is very small, i.e., near freeze-out. At the same time, the formation of the bound two nucleon state requires the pres-

ence of a third body to conserve energy and momentum. This introduces a delicate dependence of the formation and survival probability of the (anti)deuteron on the size and density profile of the source.

It is of particular interest to study the production of antideuterons and the associated freeze-out volume. Antideuterons are all produced in the collision, and the production rate will thus depend on the production and annihilation probabilities of antiparticles in the medium. Additionally, antideuterons have no contribution from spectator fragments, thus guaranteeing a measurement of the participant source volume. This Letter reports on the first systematic measurement of antiproton and antideuteron yields at nonzero transverse momenta from 158A GeV/c Pb + Pb central collisions at the CERN SPS accelerator. Earlier measurements from Si + Au at the AGS and for minimum bias and $p_t = 0$ Pb + Pb (SPS) are reported in Refs. [3–5].

In a simple coalescence approach [6,7], composite particles are formed only if the constituent particles are close in phase space at freeze-out. The invariant cross section of the cluster is then expressed as the product of the invariant cross sections of the constituents. For deuterons, assuming that the (unmeasured) neutron invariant cross section has the same form, as a function of transverse momentum, as

the protons, this may be written as

$$E_d \frac{d^3 N_d}{dp_d^3} = B_2 \left(E_p \frac{d^3 N_p}{dp_p^3} \right)^2, \quad (1)$$

where $p_d = 2p_p$. This relation defines the coalescence parameter B_2 which may be experimentally determined and can be related (albeit in a model dependent way) to the volume of the emitting source. In a fireball model with chemical and thermal equilibrium [8,9],

$$B_2 = \frac{3}{4} R_{np} \frac{(hc)^3}{V} \frac{m_d}{m_p^2}, \quad (2)$$

where R_{np} is the ratio of neutrons to protons in the colliding system, and V is the volume of the fireball when the particles coalesce. The radius of the system can be calculated from

$$R^3 = \alpha R_{np} (\hbar c)^3 \frac{m_d}{m_p^2} (B_2)^{-1}, \quad (3)$$

where α is a factor that depends on the assumed source geometry, e.g., $\alpha = (9/2)\pi^2$ for a hard sphere and $\alpha = (3/4)\pi^{3/2}$ for a Gaussian source. For antideuterons, it is reasonable to assume that the ratio of antineutrons to antiprotons prior to coalescence is close to 1, whereas for deuterons R_{np} will depend upon the beam and target nuclei, as well as other details of the reaction.

The data presented here were obtained from 158A GeV/c Pb ions impinging upon a 3.8 mm Pb target and were taken during the 1996 Pb beam running period at the CERN SPS. Antiprotons and antideuterons were measured in the same rapidity range ($1.9 \leq y \leq 2.1$). The antideuteron measurement was made in the transverse momentum range from 0.8 to 1.5 GeV/c, and the antiproton (p_t) at half that of the antideuteron. For both data sets, a trigger requiring events from approximately the most central 20% of the geometric cross section was used, by measuring the total pulse height from charged particles hitting two scintillators downstream from the target and covering $1.3 \leq \eta \leq 3.5$ in pseudorapidity. Further off-line centrality selection also used these scintillators. Details of the spectrometer as employed may be found in [1]. In that paper, two hodoscopes far from the target (H3 at 18 m, $\sigma_{\text{TOF}} \approx 90$ ps, and H4 at 25 m, $\sigma_{\text{TOF}} \approx 100$ ps) were used to obtain independent measures of particle time of flight (TOF). For the antiprotons, the TOF was sufficient to uniquely and cleanly determine particle identity, whereas, to identify the rare antideuterons, an energy measurement from a calorimeter (UCAL) was also required.

Acceptance effects and tracking inefficiencies have been corrected via a Monte Carlo procedure. The data have also been corrected for those events in which an antiproton or heavier particle is vetoed by a pion in the spectrometer in the same event using the method detailed in [10]. The antideuteron results include a correction for the efficiency of the calorimeter which is estimated to be 80%. All data have been corrected for the trigger efficiency (83%).

The square of the invariant mass (m^2) as determined by H3 is plotted against the m^2 as determined by H4 in Figs. 1a–1c. Figure 1a shows all data taken at a nominal spectrometer momentum setting of 8 GeV/c, before the imposition of any cuts. In Fig. 1b, additional restrictions in the analysis on track quality, single interaction in the target, and fiducial cuts have been applied. Such cuts remove considerable background in the region where the antideuterons are expected. Figure 1c shows the m^2 distribution obtained after also requiring

$$E_{\text{obs}}^{\text{UCAL}} \geq E_{\text{kin}} + E_{\text{anhi}} - 2\sigma_{\text{UCAL}}, \quad (4)$$

where $E_{\text{obs}}^{\text{UCAL}}$ is the experimentally observed energy deposit in the UCAL, E_{kin} is the experimentally determined kinetic energy, E_{anhi} is the energy liberated in the annihilation of a \bar{d} , and σ_{UCAL} is the energy resolution of the UCAL. It can be seen that this requirement selects the heavy antiparticles and removes the background of misidentified particles. Antideuterons are now clearly visible at about $m_d^2 = 3.5$ GeV²/c⁴. Figure 1(d) shows the m^2 distribution, requiring that a consistent TOF (within $\pm 2\sigma$) be measured in both H3 and H4. The unfilled histogram corresponds to the data in Fig. 1b, while the filled histogram presents the data after the UCAL cut. A total of 24 antideuterons are identified in the m^2 interval from 3 to 4 GeV²/c⁴, of which 20 remain after fiducial cuts.

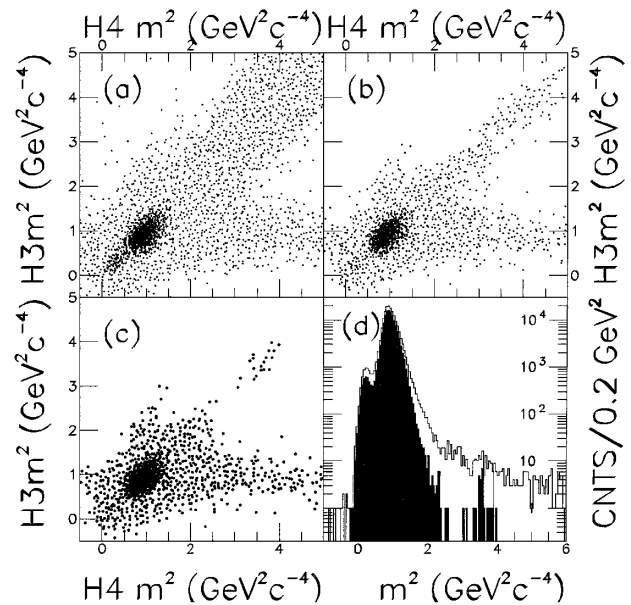


FIG. 1. (a) Mass squared as determined in time of flight hodoscope H3 versus the similar quantity determined for hodoscope H4. (b) Same as panel (a) but with cuts on track quality and rejecting multiple interactions in the target. (c) Same as panel (b) but further requiring that the measured energy in the calorimeter is greater than the sum of the kinetic energy of the particle and the annihilation energy less twice the calorimeter resolution. (d) Distribution of particles versus m^2 , requiring consistent TOF in both H3 and H4, before (unfilled) and after (filled) imposition of the UCAL cut. Antideuterons are recognized as the isolated peak centered at $m^2 = 3.54$ GeV²/c⁴.

The antideuterons measured at the 8 GeV/c setting fall in the transverse momentum (p_t) range $0.6 \leq p_t \leq 1.6$ GeV/c, and in the rapidity interval 1.9 to 2.1. Antiprotons measured at the 4 GeV/c setting fall in the same rapidity interval and in the range $0.3 \leq p_t \leq 0.8$ GeV/c. Off-line fiducial cuts restrict the range to be from 0.8 (0.4) to 1.5 (0.75) GeV/c for antideuterons (antiprotons). The invariant cross section $(1/\sigma_{\text{trig}})Ed^3\sigma/dp^3$ for the antideuterons is presented as a function of transverse momentum in Fig. 2a. The mean transverse momentum of the antideuteron distribution within the spectrometer acceptance is consistent with that of deuterons. The deuteron inverse slope parameter is 385 ± 20 MeV [11,12]. The antiproton spectrum is presented in Fig. 2a as a function of $p_t(\bar{d})$ [i.e., $2p_t(\bar{p})$]. The inverse slope parameter obtained from an exponential fit to the transverse mass spectrum of the antiprotons is $T = 300 \pm 25$ MeV.

The coalescence parameter for antideuterons is plotted as a function of $p_t(\bar{d})$ in Fig. 2b. The average value for the most central 10% of the cross section is $B_2(\bar{d}) = (1.8 \pm 0.5) \times 10^{-4}$ GeV²/c³ as shown by the solid line in Fig. 2b. It should be noted, however, that antiprotons originating from weak decays of strange baryons (e.g., $\bar{\Lambda}$) contribute to the measured antiproton yield in the NA44 spectrometer acceptance and cannot be distinguished from

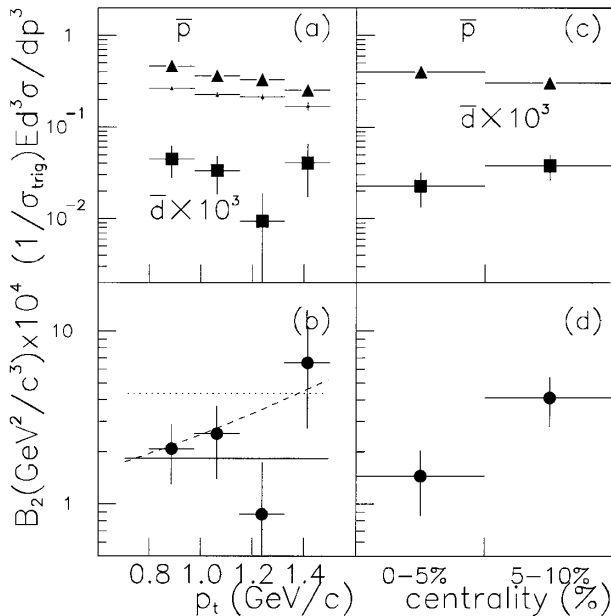


FIG. 2. (a) Antiproton (triangles) and antideuteron (squares) yields and (b) B_2 as a function of the antideuteron transverse momentum. The small symbols in (a) are the antiproton points corrected for weak decays. In (b), the solid line is the average B_2 while the dashed line is the calculated B_2 assuming an antideuteron inverse slope of 400 MeV. The dotted line is the average B_2 , after correcting for contributions from weakly decaying strange baryons (see text for details). Yields versus centrality for two centrality bins (c); the first bin is the 5% most central data and the second is 5–10% central. (d) B_2 for these two centrality bins.

primary antiprotons. Figure 2a shows the antiprotons with and without the weak decay correction. The correction factor has been calculated using the event generator RQMD 2.3 [13] to provide input for a Monte Carlo simulation of the NA44 spectrometer. RQMD ratios for strange particles have been found to be consistent with NA44 kaon data [14] and preliminary ratios from WA97 [15] and NA49 [16]. The effect of the correction is to decrease the antiproton yield, thus increasing B_2 (where the correction appears squared) with respect to the uncorrected value, as can be seen in Fig. 2b.

Particle yields in two centrality bins, corresponding to the 5% and 5%–10% most central collisions, are shown in Fig. 2c, where the \bar{p} cross section has not been corrected for weak decay products. The \bar{p} cross section increases with centrality while the \bar{d} yield decreases. This is reflected in the B_2 (Fig. 2d) which decreases with centrality at the 1.5σ level. If $\bar{\Lambda}/\bar{p}$ is constant as a function of centrality, the corrected B_2 will decrease by 2.7 ± 1.3 , somewhat more than expected for the geometrical increase in collision volume of roughly 30%.

In Fig. 3 we plot B_2 for both deuterons (open symbols) and antideuterons (solid symbols), for a variety of other systems and beam energies [3,5,17–26], and this paper. The present result for the most central 10% of the cross section is plotted as the larger solid circle and the corrected value as a smaller solid circle. B_2 decreases with increasing beam energy and system size for $A + A$ collisions, suggesting increasing freeze-out volumes. The present measurement of B_2 for antideuterons is found to be

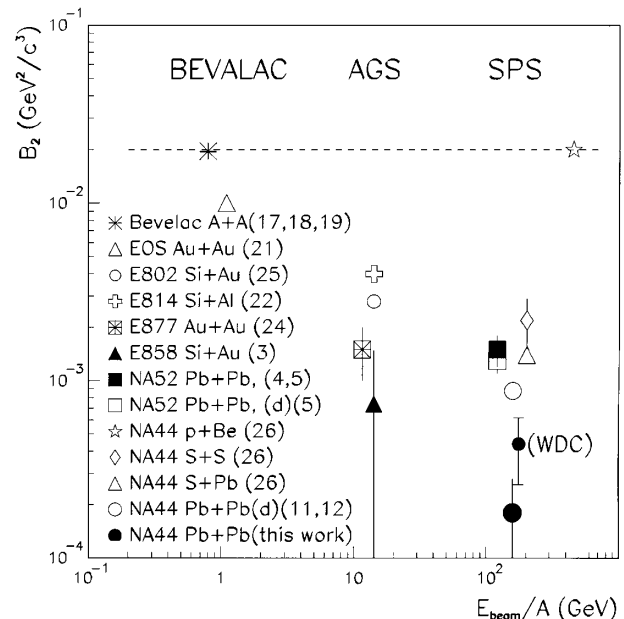


FIG. 3. Comparison of B_2 for deuterons (open symbols) and antideuterons (solid symbols). The solid line represents the systematics of $p + p$ and $p + A$ collisions. The larger solid circle is from this work. The smaller solid circle includes the calculated correction for weak decays; the other points do not.

close to the corresponding value for deuterons, suggesting that the coalescence dynamics for antibaryon clusters and baryon clusters are similar.

For deuterons at AGS [25] and SPS [11,12] energies, B_2 increases with increasing transverse momentum. The present antideuteron data are consistent with this trend. Such an increase can be understood as arising from the dynamics of the expansion. Polleri *et al.* [27] have shown that the p_t dependence of B_2 is related to the density profile of the source at freeze-out and on the functional form of the transverse expansion velocity as a function of radius. An increase in B_2 with increasing p_t is consistent with a source with a sharp surface and a near-linear transverse expansion profile, whereas with this expansion profile a Gaussian density profile leads to a B_2 essentially independent of p_t .

Finally, assuming a source with a sharp surface, we obtain from the present data, corrected for weak decays and using Eq. (3), a source radius parameter of $R = 11.6 \pm 1$ fm. This value can be compared with typical HBT radii extracted from two meson correlation functions. These radii are about 4 fm, when scaled assuming a dependence proportional to $m_t^{-1/2}$ to the transverse mass of the coalescing particles ($\langle m_t \rangle = 1.1$ GeV/ c) [1]. However, the HBT radii are obtained assuming Gaussian source distributions, and should be rescaled by a (purely geometrical) factor of $(6\sqrt{\pi})^{1/3} = 2.2$, yielding a good agreement between two particle coalescence and two particle HBT data.

In summary, we have presented the first measurement of antideuterons at nonzero p_t from Pb + Pb collisions at CERN SPS energies. This result, together with the measured yield of antiprotons in the same rapidity range, has allowed us to extract a coalescence parameter $B_2(\vec{d}) = (1.8 \pm 0.5) \times 10^{-4}$ GeV²/ c^3 for the 10% most central collisions. After corrections for contribution from weakly decaying strange baryons, we obtain a value of $(4.4 \pm 1.3) \times 10^{-4}$ GeV²/ c^3 .

This work has been supported by the Danish Natural Science Research Council, the Japanese Society for the Promotion of Science, the Japanese Ministry of Education, Science, and Culture, the Swedish Science Research Council, the Fond für Förderung der Wissenschaftlichen

Forschung, the National Science Foundation, and the U.S. Department of Energy.

*Now at Heidelberg University, D-69120 Heidelberg, Germany.

†Now at Brookhaven National Laboratory, Upton, NY 11973.

‡Now at Lawrence Berkeley National Laboratory, Berkeley, CA 94720.

§Deceased.

||Now at Wayne State University, Detroit, MI 48201.

**Institute of Physics, Warsaw University of Technology, Koszykowa 75, 00-662 Warsaw, Poland.

††Now at Osaka University, Toyonaka, Osaka 560-0043, Japan.

- [1] I. G. Bearden *et al.*, Phys. Rev. C **58**, 1656 (1998).
- [2] W. Zajc, Nucl. Phys. **A630**, 511c (1998).
- [3] M. Aoki *et al.*, Phys. Rev. Lett. **69**, 2345 (1992).
- [4] G. Appelquist *et al.*, Phys. Lett. B **376**, 245 (1996).
- [5] G. Ambrosini *et al.*, Phys. Lett. B **417**, 202 (1998).
- [6] S. F. Butler and C. A. Pearson, Phys. Rev. **129**, 836 (1963).
- [7] A. Schwarzschild and C. Zupancic, Phys. Rev. **129**, 854 (1963).
- [8] A. Z. Mekjian, Phys. Rev. C **17**, 1051 (1978).
- [9] L. P. Csernai and J. I. Kapusta, Phys. Rep. **131**, 223 (1986).
- [10] I. G. Bearden *et al.*, Phys. Lett. B **388**, 431 (1996).
- [11] A. G. Hansen, Ph.D. thesis, University of Copenhagen, 1999.
- [12] A. G. Hansen *et al.*, Nucl. Phys. **A661**, 387c (1999).
- [13] H. Sorge, Phys. Rev. C **52**, 3291 (1995).
- [14] I. G. Bearden *et al.*, Phys. Lett. B **471**, 6 (1999).
- [15] E. Andersen *et al.*, Nucl. Phys. **A638**, 115c (1998).
- [16] H. Appelshäuser *et al.*, Nucl. Phys. **A638**, 91c (1998).
- [17] S. Nagamiya *et al.*, Phys. Rev. C **24**, 971 (1981).
- [18] H. H. Gutbrod *et al.*, Phys. Rev. Lett. **37**, 667 (1976).
- [19] R. L. Auble *et al.*, Phys. Rev. C **28**, 1552 (1983).
- [20] J. W. Cronin *et al.*, Phys. Rev. D **11**, 3105 (1975).
- [21] S. Wang *et al.*, Phys. Rev. Lett. **74**, 2646 (1995).
- [22] J. Barrette *et al.*, Phys. Rev. C **50**, 1077 (1994).
- [23] J. Barrette *et al.*, Phys. Rev. C **50**, 3047 (1994).
- [24] S. C. Johnson, Ph.D. thesis, SUNY Stony Brook, 1997.
- [25] T. Abbot *et al.*, Phys. Rev. C **50**, 1024 (1994).
- [26] J. Simon-Gillo, Nucl. Phys. **A590**, 483c (1995).
- [27] A. Polleri *et al.*, Phys. Lett. B **419**, 19 (1998).